Research Article

Journal of MASS SPECTROMETRY

Received: 11 November 2011 Revised: 27 December 2011 Accepted: 4 January 2012 Published online in Wiley Online Library

(wileyonlinelibrary.com) DOI 10.1002/jms.2954

Identification and characterization of proanthocyanidins of 16 members of the *Rhododendron* genus (*Ericaceae*) by tandem LC–MS

Rakesh Jaiswal,[a] Lalith Jayasinghe[b] and Nikolai Kuhnert[a]*

ABSTRACT: The proanthocyanidins of the leaves of 16 taxa of the *Rhododendron* genus (*Ericaceae*) [*Rhododendron* 'Catawbiense Grandiflorum', *Rhododendron* 'Cunningham's White', *Rhododendron smirnowii* Trautv., *Rhododendron calophytum* Franch., *Rhododendron dichroanthum* ssp. *scyphocalyx* (Balf. f. & Forrest) Cowan, *Rhododendron micranthum* Turcz., *Rhododendron praevernum* Hutch., *Rhododendron ungernii* Trautv., *Rhododendron kaempferi* Planch., *Rhododendron degronianum* ssp. *heptamerum* var. *hondoense* (Nakai) H. Hara, *Rhododendron fortunei* Lindl., *Rhododendron ponticum* L., *Rhododendron galactinum* Balf. f. ex Tagg., *Rhododendron oreotrephes* W. W. Sm., *Rhododendron brachycarpum* ssp. *brachycarpum* D. Don ex G. Don, and *Rhododendron insigne* Hemsl. & E. H. Wilson] were investigated qualitatively by liquid chromatography–mass spectrometry in series. Twenty-nine dimeric proanthocyanidins based on (epi)catechin and (epi)gallocatechin were detected and characterized on the basis of their unique fragmentation pattern in the negative ion mode tandem mass spectrometry spectra. All of them were extracted for the first time from these sources, and ten of them were not reported previously in nature. The position of the galloyl residue was assigned on the basis of the retro-Diels–Alder fragmentation and the dehydrated retro-Diels–Alder fragmentation; it resulted from the loss of gallic acid as a neutral loss in the negative ion mode. Furthermore, four caffeoylquinic acids, six *p*-coumaroylquinic acids, epigallocatechin, gallocatechin, catechin, epicatechin, epigallocatechin gallate, catechin gallate, epicatechin gallate, gallocatechin gallate, two quercetin-*O*-hexosides, quercetin-*O*-galloyl-hexoside, quercetin-*O*-pentoside, quercetin-*O*-rhamnoside, quercetin-*O*-pentoside-*O*-hexoside, quercetin-*O*-rhamnoside-*O*-hexoside, quercetin-*O*-feruloyl-hexoside, quercetin-*O*-(*p*-hydroxy)benzoyl-hexoside, taxifolin-*O*-pentoside, myricetin-*O*-rhamnoside, two myricetin-*O*-pentosides, three myricetin-*O*-hexosides, and two myricetin-*O*-galloyl-hexosides were detected and shown to possess characteristic tandem mass spectrometry spectra and were tentatively assigned on the basis of their retention time.

Keywords: proanthocyanidins; glycosides; *Rhododendron*; polyphenols; *Ericaceae*; tandem MS

INTRODUCTION

Proanthocyanidins (PAs) are oligomers and polymers of flavan-3-ol units such as afzelechin, epiafzelechin, catechin, epicatechin, gallocatechin, and epigallocatechin (Fig. 1). These PAs are the second-most abundant natural phenolics after lignin.[1] PAs are present in many vegetables, fruits,[2–4] beverages,[5,6] and grains[7] and are claimed to have potential antioxidant,[8,9] anticancer,[10] antimutagenic,[11,12] antidiabetic,[13] anti-inflammatory,[14,15] and anti-HIV[16] properties. PAs are also beneficial for wound healing,[17] reduce the risks of cardiovascular diseases[18–20] and skin diseases,[21] and protect from drug toxicity,[22] ultraviolet (UV) radiations,[23,24] and asthma.[25]

The natural occurrence and structural chemistry of PAs have been reviewed by Scalbert and Santos-Buelga.[26] Even today, more than 70 years after their initial discovery by Masqualier,[27] structure elucidation of PAs poses a significant and unsolved challenge to natural product chemists. This challenge can be traced back to the large structural variations defined by aspects of regiochemistry and stereochemistry encountered in PAs. In PAs, three stereogenic carbons are present at C2, C3, and C4 of each benzopyran heterocyclic moiety. If the 2,3 stereochemistry is *trans*, the monomer is designated as catechin, whereas if the 2,3 stereochemistry is *cis* , the monomer is designated as epicatechin. Galloylation has been frequently reported, with the 3-OH being the most common site of galloylation. Further ether linkages have been observed producing A-type PAs.

Additionally, chromatographic methods are only able to resolve PAs by size on normal-phase columns and by isomerism on reverse-phased packing, but never both at the same time, making the availability of a complete set of reference compounds so far impossible.[26] In terms of regiochemistry, two flavan-3-ols of different oxygenation patterns can give rise to four different isomer permutations, a topic that has been partially resolved by the group of Deinzer using a positive ion mode tandem mass spectrometry (MS) sequencing protocol and further work by Gu.[28,29] In this contribution, we expand on this approach by using negative ion mode sequencing more suitable for PAs because they ionize more

* *Correspondence to: Nikolai Kuhnert, Chemistry, Jacobs University Bremen. Email: n.kuhnert@jacobs-university.de*

a *School of Engineering and Science, Chemistry, Jacobs University Bremen, Campus Ring 8, 28759 Bremen, Germany*

b *Institute of Fundamental Studies, Hantana Road, Kandy, Sri Lanka*

Journal of MASS SPECTROMETRY

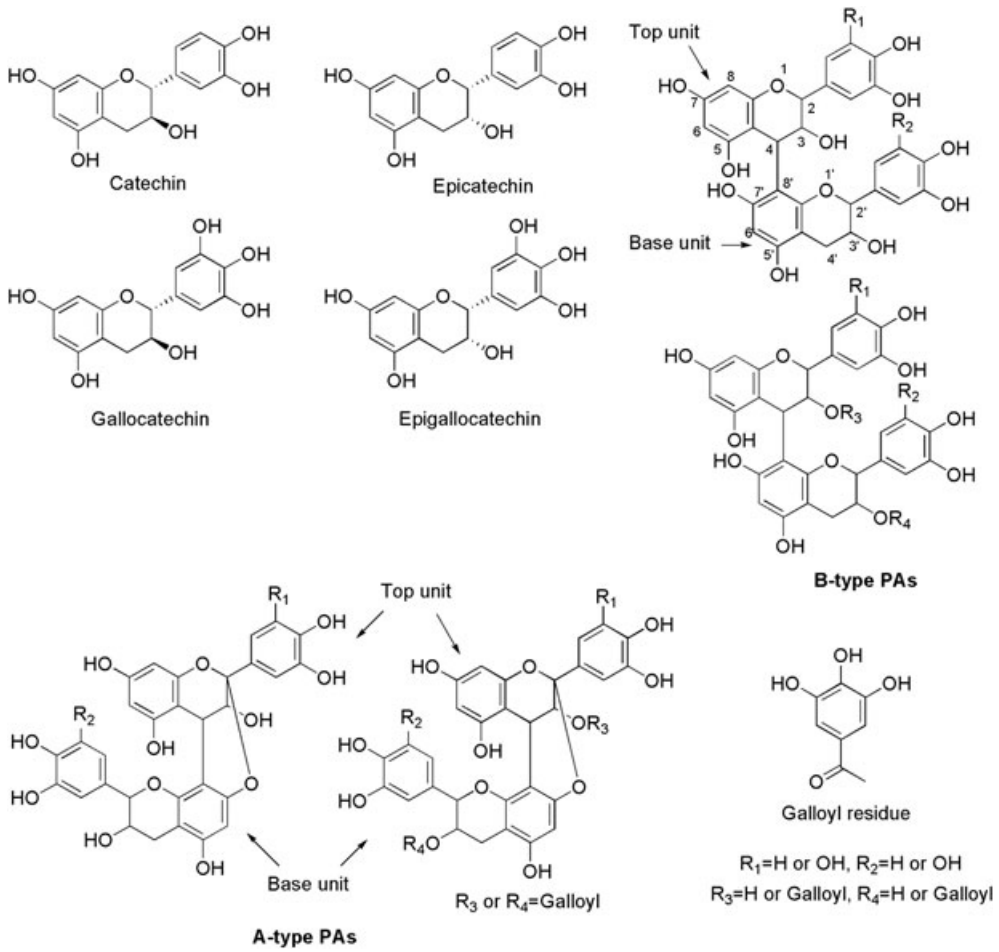

Figure 1. Representative structures of flavan-3-ol units and PAs of *Rhododendron*.

efficiently in this ion mode. A further unresolved issue of regiochemistry in the dimerization of two flavan-3-ols of the same oxygenation pattern (e.g., two catechins) involves the formation of either 4–8 or 6–8 linkage. In terms of stereochemistry, two flavan-3-ols can in theory form eight stereoisomers with either 4–8 or 4–6 linkage each, with so far only compounds of 3,4-*trans* stereochemistry observed in nature. To resolve the issue of assignment of both regiochemistry and stereochemistry in PAs, it is of utmost importance to identify natural sources that biosynthesize a maximum number of isomeric compounds to allow direct comparison of, for example, fragment spectra of as many isomers as possible to identify differences in fragmentation patterns and hence deduce rules and patterns for structure assignment. In this contribution, we show that plants of the genus *Rhododendron* are an exceptionally rich source of PAs, especially in terms of numbers of isomeric compounds produced, which in many cases reach the theoretical maximum. Therefore, *Rhododendron* analysis opens up new avenues in PA structure elucidation.

The genus *Rhododendron* is distributed throughout the globe with the exception of South and Middle America and Africa, growing in a large variety of climatic conditions. The genus *Rhododendron*, belonging to the *Ericaceae* family of plants, comprises more than 1000 botanically identified species and close to 30 000 different cultivars. Therefore, it constitutes the plant genus with one of the highest species diversity. *Rhododendrons* are best known for their use in gardens for ornamental purposes. The phytochemical profile of only a few species of *Rhododendron* has been investigated so far. These taxa are a source of phenolic compounds, especially flavonoids[28] and their glycosides,[29–34] essential oils,[35,36] chromones,[37] chromanes and chromenes,[38] β-diketones,[39] iridoids,[40] terpenoids,[41–44] and steroids.[45] Medicinal use of *Rhododendron*-plant-derived formulations is restricted because of the occurrence of phytotoxins called grayanotoxins, a class of terpenoids present in many plants of this genus and family.[43,46] However, some plants of this genus, low in grayanotoxins, are used for medicinal purposes in Turkish,[15] Chinese,[43,47] homeopathic,[48] and ayurvedic[49] medicinal systems to treat chronic diseases. *Rhododendron* plants are also reported to have antioxidant,[50,51] anti-inflammatory,[15] antiviral,[38,52] and hepatoprotective properties[49] due to their phenolic constituents.

In this study, all the PAs, *O*-glycosides of flavonoids, and hydroxycinnamates analyzed were extracted from the leaves of a botanically representative selection of two cultivars and 14 species of *Rhododendron*, representing a variety of geographical origins, including *Rhododendron smirnowii* Trautv., *Rhododendron calophytum* Franch., *Rhododendron dichroanthum* ssp. *scyphocalyx* (Balf. f. & Forrest) Cowan, *Rhododendron micranthum* Turcz., *Rhododendron praevernum* Hutch., *Rhododendron ungernii* Trautv., *Rhododendron kaempferi* Planch., *Rhododendron degronianum* ssp. *heptamerum* var. *hondoense* (Nakai) H. Hara, *Rhododendron fortunei* Lindl., *Rhododendron ponticum* L., *Rhododendron galactinum* Balf. f. ex Tagg., *Rhododendron oreotrephes* W. W. Sm., *Rhododendron brachycarpum* ssp. *brachycarpum* D. Don ex G. Don, *Rhododendron insigne* Hemsl. & E. H. Wilson, *Rhododendron* 'Catawbiense

Grandiflorum', and *Rhododendron* 'Cunningham's White'. The compounds were identified qualitatively without any purification or isolation, and assignment was based on their liquid chromatography (LC)–MS^n behavior.

EXPERIMENTAL

Chemicals and materials

All the chemicals (analytical grade) were purchased from Sigma-Aldrich (Bremen, Germany). The PAs, B1, and B2 were purchased from PhytoLab (Vestenbergsgreuth, Germany). Green fresh leaves of all the 16 plants were collected from the Botanic Garden and Rhododendron-Park Bremen (Germany) in spring season. Plants have been identified, and records (vouchers) of their botanical origin and identity are kept at the Botanic Garden and Rhododendron-Park Bremen under the scientific supervision of Dr Hartwig Schepker.

Sample preparation

Green leaves (5 g) of each plant were freeze-dried at −20 °C overnight, extracted with aqueous methanol (100 ml, 70%), homogenized with a blender, and ultra-sonicated for 10 min. These extracts were filtered through a Whatman no. 1 filter paper. The solvents were removed by evaporation *in vacuo*, and the extracts were stored at −20 °C until required, thawed at room temperature, dissolved in methanol (120 mg/10 ml of methanol), filtered through a membrane filter, and used directly for LC–MS.

Liquid chromatography–mass spectrometry in series

The LC equipment (Agilent 1100 series, Bremen, Germany) comprised a binary pump, an auto-sampler with a 100-µl loop, and a diode array detector with a light-pipe flow cell (recording at 254, 280, and 320 nm and scanning from 200 to 600 nm). This was interfaced with an ion-trap mass spectrometer fitted with an electrospray ionization source (Bruker Daltonics HCT Ultra, Bremen, Germany) operating in full-scan, auto-MS^n mode to obtain fragment ion *m/z*. Tandem mass spectra were acquired in auto-MS^n mode (smart fragmentation) using a ramping of the collision energy. Maximum fragmentation amplitude was set to 1 V, starting at 30% and ending at 200%. MS operating conditions (negative mode) had been optimized using B1-type and B2-type PAs with a capillary temperature of 365 °C, a dry gas flow rate of 10 l/min, and a nebulizer pressure of 10 psi. High-resolution LC–MS was performed using the same high-performance LC equipped with a micrOTOF mass spectrometer (Bruker Daltonics, Bremen, Germany) fitted with an electrospray ionization source, and internal calibration was achieved with 10 ml of 0.1 M sodium formate solution injected through a six-port valve prior to each chromatographic run. Calibration was performed using the enhanced quadratic mode.

High-performance liquid chromatography

Separation was achieved on a 250 × 3 mm-inner-diameter column containing 5 µm C18 amide, with a 5 mm × 3 mm-inner-diameter guard column (Varian, Darmstadt, Germany). Solvent A was water/formic acid (1000 : 0.05 v/v), and solvent B was methanol. Solvents were delivered at a total flow rate of 500 µl/min. The gradient profile was from 10% B to 70% B linearly in 60 min followed by 10 min isocratic and a return to 10% B at 90 and 10 min isocratic to re-equilibrate.

RESULTS AND DISCUSSION

The methanolic extracts of all the plants leaves were prepared to get an efficient extraction of phenolics especially PAs. These extracts were analyzed by reversed-phase high-performance LC using the diphenyl and the C18 amide columns, and it was found that the C18 amide column is more efficient in separating PAs and hydroxycinnamates than the diphenyl column. All the retention times and the MS data were collected using the C18 amide column. The elution order of the monoacyl chlorogenic acids was 3 > 4 > 5, which is completely different than that for the diphenyl column (3 > 5 > 4).[53,54] For the LC–MS measurements, negative ion mode was used to obtain better tandem mass spectra and high-resolution mass spectra. For all the compounds, the high-resolution mass data were in good agreement with the theoretical molecular formulas, all displaying a mass error of below 5 ppm, thus confirming their elemental composition. In general, peak identities were consistent both within and between analyses. However, when the mass spectrum for a particular substance included two ions of similar mean intensities, within-analysis experimental error dictated that in some individual MS scans one would be more intense, whereas for other scans, the reverse would be true. This phenomenon was encountered primarily when the signal intensity was lower, that is, with quantitatively minor components and/or higher-order spectra. For example, some of the PAs produce MS^2 ions at *m/z* 407 and 425, which are essentially coequal in some spectra. However, in this particular case, the lower mass ion was assigned consistently as the base peak. Fragment ions with intensities <10% of the base peak were reported only when they were needed for comparison.

In the following section, we discuss in detail the identity of the PAs identified in the 16 plants under investigation. In this contribution, we focus exclusively on dimeric PAs. In terms of PA nomenclature, we use the system suggested by Porter.[55] Here, for dimeric structures, the catechin unit bearing a catechin substituent at the C-4 position of its C-ring is designated as the top unit, whereas the C-4′ unsubstituted catechin unit is designated as the base unit. Numbering of the catechin rings follows the regular International Union of Pure and Applied Chemistry system with the base unit carbons designated by a dash. Not all of the identified PAs were observed in all the samples (Table 1). The detailed phytochemical profile of the 16 plants under investigation is given in Table 2.

The phenolics were positively identified by their typical UV absorptions at 254, 280, and 320 nm. All the glycosides showed the neutral loss of the glycone part; hydroxycinnamates showed loss of the cinnamoyl/cinnamic acid part; PAs showed loss of the galloyl/gallic acid part and the Diels–Alder fraction in the negative ion mode.

For positive identification and characterization of PAs, the following points were considered:

1. UV spectrum at 280 nm (λ_{max}).
2. Molecular ion peaks (M-H) in negative ion mode of MS, for example, *m/z* 577, 593, 729, and 745 for B-type PAs and 575, 591, 721, and 743 for A-type PAs.
3. The fragmentation pathway described by Gu *et al.*, for example, heterocyclic ring fission (HRF) and retro-Diels–Alder (RDA)

Table 1. Presence of proanthocyanidins, glycosides, and hydroxycinnamates in the plants of *Rhododendron* genus

No.	Compound	R1	R2	R3	R4	R5	R6	R7	R8	R9	R10	R11	R12	R13	R14	R15	R16
1	(Epi)catechin-(4,8′)-(epi)catechin (B1)	Y	Y	Y	Y	Y	Y	Y	Y	Y	Y	Y	—	—	Y	Y	Y
2	(Epi)catechin-(4,8′)-(epi)catechin	Y	Y	Y	Y	Y	Y	Y	Y	Y	Y	Y	Y	—	Y	Y	Y
3	(Epi)catechin-(4,8′)-(epi)catechin	Y	Y	Y	Y	Y	Y	Y	—	Y	Y	Y	—	—	Y	Y	Y
4	(Epi)catechin-(4,8′)-(epi)catechin (B2)	Y	Y	Y	Y	Y	Y	—	Y	—	Y	Y	—	—	Y	Y	Y
5	(Epi)catechin-(4,8′)-(epi)catechin	—	Y	Y	Y	Y	—	Y	—	Y	Y	—	—	—	Y	Y	Y
6	(Epi)catechin-(4,8′)-(epi)catechin	Y	Y	Y	Y	Y	Y	Y	Y	Y	Y	Y	—	—	Y	Y	Y
7	(Epi)catechin-(4,8′)-(epi)catechin	Y	Y	Y	Y	—	Y	Y	—	Y	—	—	—	—	Y	—	Y
8	(Epi)gallocatechin-(4,8′)-(epi)catechin	Y	Y	—	—	—	—	—	Y	—	—	—	—	—	—	Y	—
9	(Epi)gallocatechin-(4,8′)-(epi)catechin	Y	Y	—	—	Y	—	—	Y	—	—	—	—	—	—	Y	—
10	(Epi)catechin-(4,8′)-(epi)gallocatechin	Y	Y	—	—	Y	—	—	Y	—	—	—	—	—	—	Y	—
11	(Epi)gallocatechin-(4,8′)-(epi)catechin	Y	Y	—	—	—	Y	—	Y	—	—	—	—	—	—	Y	—
12	(Epi)catechin-(4,8′)-(epi)gallocatechin	Y	Y	—	—	—	—	—	—	—	—	—	—	—	—	—	—
13	(Epi)gallocatechin-(4,8′)-(epi)catechin	Y	Y	—	—	—	—	—	Y	—	—	—	—	—	—	—	—
14	(Epi)gallocatechin-(4,8′)-(epi)gallocatechin	Y	—	—	—	—	—	—	—	—	—	—	—	—	—	Y	—
15	(Epi)gallocatechin-(4,8′)-(epi)gallocatechin	Y	Y	—	—	—	—	—	Y	—	—	—	—	—	—	—	—
16	(Epi)gallocatechin-(4,8′)-(epi)gallocatechin	Y	Y	—	—	—	—	—	—	—	—	—	—	—	—	—	—
17	3-*O*-Galloyl(epi)catechin-(4,8′)-(epi)catechin	Y	Y	Y	—	Y	—	—	Y	—	Y	Y	—	—	—	Y	—
18	(Epi)catechin-(4,8′)-3′-*O*-galloyl-(epi)catechin	Y	Y	Y	—	Y	—	—	Y	—	Y	Y	Y	—	—	Y	—
19	3-*O*-Galloyl(epi)catechin-(4,8′)-(epi)catechin	Y	Y	Y	—	Y	—	Y	Y	—	Y	Y	Y	—	—	Y	Y
20	(Epi)catechin-(4,8′)-3′-*O*-galloyl(epi)catechin	Y	Y	—	—	Y	—	—	Y	—	Y	Y	—	—	—	Y	—
21	(Epi)gallocatechin-(4,8′)-3′-*O*-galloyl(epi)catechin	Y	—	—	—	—	—	—	Y	—	—	—	—	—	—	—	—
22	3-*O*-Galloyl(epi)catechin-(4,8′)-(epi)gallocatechin	Y	Y	—	—	—	—	—	Y	—	—	—	—	—	—	—	—
23	(Epi)gallocatechin-(4,8′)-3′-*O*-galloyl(epi)catechin	—	Y	—	—	—	—	—	Y	—	—	—	Y	—	—	—	—
24	(Epi)gallocatechin-(4,8′)-3′-*O*-galloyl(epi)gallocatechin	—	—	—	—	—	—	—	Y	—	—	—	—	—	—	—	—
25	(Epi)gallocatechin-(4,8′)-3′-*O*-galloyl(epi)gallocatechin	—	—	—	—	—	—	—	Y	—	—	—	—	—	—	—	—
26	(Epi)catechin-(4,8′/2,6′)-(epi)catechin	Y	Y	Y	Y	Y	—	—	—	—	Y	—	—	Y	Y	Y	Y
27	3-*O*-Galloyl(epi)catechin-(4,8′/2,6′)-(epi)catechin	Y	Y	Y	—	Y	—	—	Y	—	Y	—	—	Y	—	—	—
28	3-*O*-Galloyl(epi)catechin-(4,8′/2,6′)-(epi)gallocatechin	Y	Y	—	—	—	—	—	Y	—	—	—	—	—	—	—	—
29	(Epi)gallocatechin-(4,8′/2,6′)-3′-*O*-galloyl(epi)gallocatechin	Y	—	—	—	—	—	—	—	—	—	—	—	—	—	—	—
30	3-*O*-Caffeoylquinic acid	Y	—	—	—	—	Y	Y	—	Y	—	Y	Y	—	Y	—	Y
32	*Cis*-3-*O*-caffeoylquinic acid	—	—	—	Y	—	Y	Y	—	Y	—	—	—	—	Y	—	—
32	5-*O*-Caffeoylquinic acid	Y	—	—	Y	—	Y	Y	Y	Y	—	—	Y	—	Y	—	Y
33	*Cis*-5-*O*-caffeoylquinic acid	—	—	—	—	—	Y	Y	Y	Y	—	—	—	—	—	—	—
34	3-*O*-*p*-Coumaroylquinic acid	Y	—	—	—	—	Y	—	—	Y	—	Y	Y	Y	—	—	—
35	*Cis*-3-*O*-*p*-coumaroylquinic acid	Y	—	—	—	—	Y	—	—	Y	—	Y	—	—	—	—	—
36	4-*O*-*p*-Coumaroylquinic acid	—	—	—	—	—	—	Y	—	—	—	—	—	Y	—	—	—
37	*Cis*-4-*O*-*p*-coumaroylquinic acid	—	—	—	—	—	—	Y	—	—	—	—	—	Y	—	—	—
38	5-*O*-*p*-Coumaroylquinic acid	—	—	—	Y	—	Y	Y	Y	Y	—	—	—	—	—	—	—
39	*Cis*-5-*O*-*p*-coumaroylquinic acid	—	—	—	Y	—	Y	Y	Y	Y	—	—	—	—	—	—	—
40	Catechin	Y	Y	Y	Y	Y	Y	Y	Y	Y	Y	Y	Y	Y	Y	Y	Y
41	Epicatechin	Y	Y	Y	Y	Y	Y	Y	—	Y	Y	Y	—	Y	Y	Y	Y
42	Gallocatechin	Y	Y	Y	—	Y	Y	—	Y	Y	—	Y	—	—	—	Y	—
43	Epigallocatechin	Y	Y	Y	—	Y	Y	Y	—	—	—	—	—	—	Y	Y	—
44	Catechin gallate	Y	Y	Y	Y	Y	—	—	Y	—	Y	Y	Y	—	—	Y	Y
45	Epicatechin gallate	Y	Y	Y	Y	Y	—	Y	Y	—	Y	Y	Y	—	—	Y	—
46	Gallocatechin gallate	Y	Y	Y	—	—	—	—	—	—	—	—	Y	—	—	—	—
47	Epigallocatechin gallate	Y	Y	Y	—	—	—	—	Y	—	—	—	—	—	—	Y	—
48	Quercetin-*O*-hexoside	Y	Y	Y	Y	Y	Y	Y	Y	Y	Y	Y	Y	Y	Y	Y	Y
49	Quercetin-*O*-hexoside	—	Y	—	—	—	—	—	—	—	—	—	—	—	—	—	—
50	Quercetin-*O*-galloyl-hexoside	Y	Y	Y	—	Y	—	—	Y	—	—	—	Y	—	—	Y	Y
51	Quercetin-*O*-pentoside	Y	Y	Y	Y	Y	Y	Y	Y	Y	Y	Y	Y	Y	Y	Y	Y
52	Quercetin-*O*-rhamnoside	Y	Y	Y	Y	Y	Y	Y	Y	Y	Y	Y	Y	Y	Y	Y	Y
53	Quercetin-*O*-pentoside-*O*-hexoside	Y	Y	—	Y	—	—	—	—	—	—	—	—	—	—	—	—
54	Quercetin-*O*-rhamnoside-*O*-hexoside	Y	—	Y	Y	Y	—	Y	Y	—	—	Y	Y	Y	Y	Y	Y
55	Quercetin-*O*-rhamnoside-*O*-hexoside	Y	—	Y	Y	Y	—	—	Y	—	—	Y	Y	Y	Y	Y	Y
56	Quercetin-*O*-feruloyl-hexoside	Y	Y	Y	Y	Y	—	—	Y	—	—	Y	Y	Y	—	Y	Y
57	Quercetin-*O*-(*p*-hydroxy)benzoyl-hexoside	Y	Y	Y	Y	Y	—	Y	Y	—	Y	—	—	Y	Y	Y	Y

(Continues)

Table 1. *(Continued)*

No.	Compound	R1	R2	R3	R4	R5	R6	R7	R8	R9	R10	R11	R12	R13	R14	R15	R16
58	Taxifolin-*O*-pentoside	Y	Y	Y	—	Y	—	Y	Y	Y	Y	Y	Y	—	—	Y	Y
59	Myricetin-*O*-rhamnoside	Y	—	—	—	—	—	Y	Y	Y	—	Y	Y	—	—	—	—
60	Myricetin-*O*-pentoside	—	Y	—	—	—	—	—	—	—	—	—	—	—	—	Y	—
61	Myricetin-*O*-pentoside	—	Y	—	—	—	Y	—	—	—	—	—	—	—	—	—	—
62	Myricetin-*O*-hexoside	Y	Y	—	—	—	—	—	—	—	—	—	—	—	—	—	—
63	Myricetin-*O*-hexoside	Y	Y	Y	Y	—	Y	—	Y	—	—	—	Y	—	—	—	—
64	Myricetin-*O*-hexoside	Y	Y	Y	—	—	Y	—	Y	Y	Y	—	Y	—	—	—	—
65	Myricetin-*O*-galloyl-hexoside	Y	—	—	—	—	—	—	—	—	—	—	—	—	—	—	—
66	Myricetin-*O*-galloyl-hexoside	Y	—	—	—	—	—	—	Y	—	—	—	—	—	—	—	—

R1 = *Rhododendron* 'Catawbiense Grandiflorum', R2 = *Rhododendron* 'Cunningham's White', R3 = *Rhododendron smirnowii*, R4 = *Rhododendron calophytum*, R5 = *Rhododendron dichroanthum* ssp. *scyphocalyx*, R6 = *Rhododendron micranthum*, R7 = *Rhododendron praevernum*, R8 = *Rhododendron ungernii*, R9 = *Rhododendron kaempferi*, R10 = *Rhododendron degronianum* ssp. *heptamerum* var. *hondoense*, R11 = *Rhododendron fortunei*, R12 = *Rhododendron ponticum*, R13 = *Rhododendron galactinum*, R14 = *Rhododendron oreotrephes*, R15 = *Rhododendron brachycarpum* ssp. *brachycarpum*, R16 = *Rhododendron insigne*, Y = presence, — = absence.

fragmentation, gives information about the hydroxylation of the B-rings and bonds between two monomeric units, and quinone methide (QM) fragmentation defines the two monomeric units and especially the base unit (Fig. 2).[29] The loss of H_2O molecule from the C-rings indicates the epicatechin unit.

The regiochemistry of galloyl residue was assigned on the basis of the loss of a gallic acid (170 Da, neutral loss) followed by a dehydrated RDA fragment (Fig. 3).

Characterization of (epi)catechin-(4,8′)-(epi)catechin (M_r 578)

Seven [M-H] peaks were detected at *m/z* 577 in the extracted ion chromatogram (EIC). Theoretically, 16 dimeric PAs are possibly derived from catechin and epicatechin; however, Scalbert proved that only compounds with a 3,4-*trans* stereochemistry occur naturally, thus reducing the theoretically possible number of compounds to eight.[26] These seven compounds were tentatively assigned as dimeric B-type PAs (**1–7**) with (epi)catechin monomeric units. All these compounds have similar MS^n fragmentation patterns with similar intensities of ions (Fig. 4). They produced the MS^2 base peak at *m/z* 407 ($[M\text{-}H^+\text{-}170\ Da]^-$) by the loss of an RDA fragment (152 Da) followed by the loss of a water molecule (18 Da); secondary peaks at *m/z* 289 ($[(epi)catechin\text{-}H^+]^-$) originate from a QM fragment, at 425 ($[M\text{-}H^+\text{-}152\ Da]^-$) from an RDA fragment, at 451 ($[M\text{-}H^+\text{-}126\ Da]^-$) from an HRF fragment, and at 559 ($[M\text{-}H^+\text{-}H_2O]^-$) from the loss of a water molecule (Fig. 2). Loss of water was only observed for five out of the seven compounds. Taking into account that all authentic reference compounds studies composed of epicatechin moieties show this loss of water, we propose that compounds having two catechin units do not show this fragmentation pathway. With the use of this hypothesis, it is possible to distinguish two PAs with 4,6′ and 4,8′ connectivity on the basis of two catechin moieties. From the aforementioned fragmentation, these PAs were assigned as isomers of dimeric (epi)catechin-(4,8′)-(epi)catechin dimer. For further evidence, B1 and B2 PAs were used as authentic standards and showed retention times and fragmentation identical to PAs **1** and **4**, respectively. On the basis of this argument, isomers **1** and **4** were assigned as B1-type and B2-type PAs and isomers **2**, **3**, and **5–7** were assigned as B-type dimers with at least one (epi)catechin unit. Although it is possible to identify dimers containing two catechin units, it is not possible to assign more precisely by tandem MS the stereochemistry of monomeric units in PAs.

Characterization of (epi)gallocatechin-(4,8′)-(epi)catechin and (epi)catechin-(4,8′)-(epi)gallocatechin (M_r 594)

Six peaks were detected at *m/z* 593 in the EIC and were tentatively assigned as dimeric B-type PAs (**8–13**) with (epi)catechin and (epi)gallocatechin monomeric units. Isomers **8**, **9**, **11**, and **13** produced similar MS^n fragmentation patterns with similar intensities of ions (Fig. 5). They produced the MS^2 base peak at *m/z* 407 ($[M\text{-}H\text{-}186\ Da]^-$) by the loss of an RDA fragment (168 Da) from the top ring of the dimer followed by the loss of a water molecule (18 Da); secondary peaks at *m/z* 289 ($[(epi)catechin\text{-}H^+]^-$) originate from a QM fragment and at 425 ($[M\text{-}H^+\text{-}168\ Da]^-$) from an RDA fragment (Fig. 2). The presence of a QM fragment at *m/z* 289 showed that the base ring is an (epi)catechin unit, and further confirmation came from the RDA fragments at *m/z* 407 ($[M\text{-}H^+\text{-}186\ Da]^-$) and 425 ($[M\text{-}H^+\text{-}168\ Da]^-$), which show that the top unit is (epi)gallocatechin (Fig. 2). The RDA fragmentation on the top unit gave a fragment ion with a larger π–π hyperconjugated system, which is energetically more favorable than the RDA on the base unit. From the preceding arguments, these PAs must have (epi)gallocatechin as the top unit and (epi)catechin as the base unit. In these isomers, a QM fragment at *m/z* 303 was not observed, or its intensity was very low. Isomers **10** and **12** produced similar MS^n fragmentation patterns with similar intensities of ions (Fig. 5). Both isomers produced the MS^2 base peak at *m/z* 423 ($[M\text{-}H^+\text{-}170\ Da]^-$) by the loss of an RDA fragment (152 Da) followed by the loss of a water molecule (18 Da); secondary peaks at *m/z* 305 ($[(epi)gallocatechin\text{-}H^+]^-$) originate from a QM fragment, at 441 ($[M\text{-}H^+\text{-}152\ Da]^-$) from an RDA fragment, at 467 ($[M\text{-}H^+\text{-}126\ Da]^-$) from the loss of an HRF fragment, and at 575 ($[M\text{-}H^+\text{-}H_2O]^-$) from the loss of a water molecule (Fig. 2). The presence of a QM fragment at *m/z* 305 showed that the base ring is an (epi)gallocatechin unit, and further confirmation came from the RDA fragments at *m/z* 423 ($[M\text{-}H^+\text{-}152\ Da]^-$) and 441 ($[M\text{-}H^+\text{-}134\ Da]^-$), which showed that the top unit is (epi)catechin (Fig. 2). From the preceding arguments, these PAs must have (epi)catechin as the top unit and (epi)gallocatechin as the base unit. In these isomers, a QM fragment at *m/z* 287 was not observed, or its intensity was very low (Fig. 5).

Table 2. Retention times and MS^2 to MS^4 fragmentation data in negative ion mode of proanthocyanidins, glycosides, and hydroxycinnamates of *Rhododendron*

No.	Compound	Retention time (min)	Parent ion [M-H] *m/z*	Characteristic *m/z* of ions in negative ion mode
1	(Epi)catechin-(4,8′)-(epi)catechin (B1)	14.2	577	$MS^2 \rightarrow$ 407 (100), 451 (21), 425 (96), 289 (32); $MS^3 \rightarrow$ 285 (100), 389 (42), 297 (47), 283 (31), 255 (27)
2	(Epi)catechin-(4,8′)-(epi)catechin	15.4	577	$MS^2 \rightarrow$ 407 (100), 451 (22), 425 (84), 289 (19) 287 (12); $MS^3 \rightarrow$ 285 (100), 389 (26), 297 (25), 283 (27), 257 (22)
3	(Epi)catechin-(4,8′)-(epi)catechin	19.8	577	$MS^2 \rightarrow$ 407 (100), 451 (24), 425 (94), 289 (24); $MS^3 \rightarrow$ 285 (100), 389 (36), 255 (37)
4	(Epi)catechin-(4,8′)-(epi)catechin (B2)	20.9	577	$MS^2 \rightarrow$ 407 (100), 451 (15), 425 (98), 289 (35); $MS^3 \rightarrow$ 285 (100), 389 (33), 255 (36)
5	(Epi)catechin-(4,8′)-(epi)catechin	21.5	577	$MS^2 \rightarrow$ 407 (100), 451 (12), 425 (98), 289 (17); $MS^3 \rightarrow$ 285 (100), 389 (24), 255 (32)
6	(Epi)catechin-(4,8′)-(epi)catechin	24.0	577	$MS^2 \rightarrow$ 407 (100), 451 (18), 425 (98), 289 (22); $MS^3 \rightarrow$ 285 (100), 389 (25), 255 (35)
7	(Epi)catechin-(4,8′)-(epi)catechin	34.0	577	$MS^2 \rightarrow$ 407 (100), 451 (18), 425 (98), 289 (23); $MS^3 \rightarrow$ 285 (100), 389 (35), 255 (28)
8	(Epi)gallocatechin-(4,8′)-(epi)catechin	8.0	593	$MS^2 \rightarrow$ 407 (100), 425 (96), 289 (23); $MS^3 \rightarrow$ 285 (100), 389 (28), 297 (31), 281 (67), 256 (27)
9	(Epi)gallocatechin-(4,8′)-(epi)catechin	10.5	593	$MS^2 \rightarrow$ 407 (100), 425 (98), 289 (21); $MS^3 \rightarrow$ 285 (100), 389 (38), 297 (21), 281 (84), 256 (31)
10	(Epi)catechin-(4,8′)-(epi)gallocatechin	11.4	593	$MS^2 \rightarrow$ 423 (100), 575 (17), 467 (17), 441 (31), 305 (36); $MS^3 \rightarrow$ 297 (100), 407 (25), 285 (41), 283 (99)
11	(Epi)gallocatechin-(4,8′)-(epi)catechin	14.5	593	$MS^2 \rightarrow$ 407 (100), 425 (98), 289 (25); $MS^3 \rightarrow$ 285 (100), 389 (25), 297 (31), 283 (29), 281 (36), 256 (32)
12	(Epi)catechin-(4,8′)-(epi)gallocatechin	18.0	593	$MS^2 \rightarrow$ 423 (100), 575 (19), 523 (17), 467 (23), 441 (29), 305 (42); $MS^3 \rightarrow$ 297 (100), 407 (17), 283 (99), 255 (32)
13	(Epi)gallocatechin-(4,8′)-(epi)catechin	19.1	593	$MS^2 \rightarrow$ 407 (100), 425 (96), 289 (13); $MS^3 \rightarrow$ 281 (100), 285 (78), 389 (45), 257 (19), 243 (26).
14	(Epi)gallocatechin-(4,8′)-(epi)gallocatechin	5.1	609	$MS^2 \rightarrow$ 423 (100), 541 (13), 441 (30), 305 (17); $MS^3 \rightarrow$ 283 (100), 405 (17), 357 (14), 297 (81), 255 (23)
15	(Epi)gallocatechin-(4,8′)-(epi)gallocatechin	6.6	609	$MS^2 \rightarrow$ 423 (100), 441 (72), 305 (26); $MS^3 \rightarrow$ 283 (100), 405 (15), 297 (98), 255 (51), 243 (33)
16	(Epi)gallocatechin-(4,8′)-(epi)gallocatechin	10.8	609	$MS^2 \rightarrow$ 423 (100), 541 (20), 441 (65), 305 (35); $MS^3 \rightarrow$ 283 (100), 405 (13), 297 (90), 255 (67), 243 (28)
17	3-*O*-Galloyl(epi)catechin-(4,8′)-(epi)catechin	20.9	729	$MS^2 \rightarrow$ 577 (100), 559 (37), 593 (26), 451 (23), 437 (15), 425 (21), 407 (55), 289 (15); $MS^3 \rightarrow$ 407 (100), 559 (12), 451 (28), 425 (31), 299 (27), 289 (54)
18	(Epi)catechin-(4,8′)-3′-*O*-galloyl-(epi)catechin	24.6	729	$MS^2 \rightarrow$ 407 (100), 577 (26), 559 (45), 451 (28); 441 (29); 289 (21); $MS^3 \rightarrow$ 285 (100), 389 (21), 297 (27), 283 (34), 257 (18)
19	3-*O*-Galloyl(epi)catechin-(4,8′)-(epi)catechin	29.0	729	$MS^2 \rightarrow$ 577 (100), 559 (32), 425 (20), 407 (52), 289 (15); $MS^3 \rightarrow$ 407 (100), 451 (45), 425 (28), 289 (25)
20	(Epi)catechin-(4,8′)-3′-*O*-galloyl(epi)catechin	37.4	729	$MS^2 \rightarrow$ 407 (100), 577 (14), 559 (33), 441 (19); 289 (10); $MS^3 \rightarrow$ 285 (100), 389 (32), 297 (25), 255 (48), 243 (36)
21	(Epi)gallocatechin-(4,8′)-3′-*O*-galloyl(epi)catechin	21.2	745	$MS^2 \rightarrow$ 407 (100), 593 (16), 575 (21), 559 (28), 467 (20), 441 (15); 423 (22), 289 (26); $MS^3 \rightarrow$ 285 (100), 389 (28), 297 (23), 283 (39), 255 (37), 243 (28)
22	3-*O*-Galloyl(epi)catechin-(4,8′)-(epi)gallocatechin	24.3	745	$MS^2 \rightarrow$ 593 (100), 575 (21), 437 (17), 425 (27), 423 (15), 407 (59), 305 (14), 289 (10); $MS^3 \rightarrow$ 289 (100), 575 (34), 467 (53), 423 (29), 407 (40), 245 (27)
23	(Epi)gallocatechin-(4,8′)-3′-*O*-galloyl(epi)catechin	20.1	745	$MS^2 \rightarrow$ 407 (100), 577 (46), 559 (79), 289 (12); $MS^3 \rightarrow$ 285 (100), 389 (19), 297 (25), 283 (33), 256 (26)
24	(Epi)gallocatechin-(4,8′)-3′-*O*-galloyl(epi)gallocatechin	14.2	761	$MS^2 \rightarrow$ 423 (100), 609 (33), 593 (26), 575 (26), 405 (14), 305 (21); $MS^3 \rightarrow$ 283 (100), 405 (25), 297 (86), 255 (47), 243 (44)
25	(Epi)gallocatechin-(4,8′)-3′-*O*-galloyl(epi)gallocatechin	16.9	761	$MS^2 \rightarrow$ 423 (100), 609 (13), 593 (28), 575 (34), 405 (11), 305 (10); $MS^3 \rightarrow$ 283 (100), 405 (32), 297 (48), 255 (37), 243 (32)
26	(Epi)catechin-(4,8′/2,6′)-(epi)catechin	28.5	575	$MS^2 \rightarrow$ 449 (100), 539 (53), 447 (32), 423 (26), 407 (33), 327 (22), 289 (39), 287 (34), 285 (29); $MS^2 \rightarrow$ 287 (100), 431 (15), 313 (20), 297 (15), 285 (27), 243 (22)
27	3-*O*-galloyl(epi)catechin-(4,8′/2,6′)-(epi)catechin	38.2	727	$MS^2 \rightarrow$ 575 (100), 557 (16), 423 (37), 303 (16), 285 (10); $MS^3 \rightarrow$ 449 (100), 539 (47), 447 (38), 407 (28), 289 (43), 287 (40), 285 (39); $MS^4 \rightarrow$ 287 (100), 405 (41), 313 (48), 273 (23)
28	3-*O*-galloyl(epi)catechin-(4,8′/2,6′)-(epi)gallocatechin	33.2	743	$MS^2 \rightarrow$ 591 (100), 573 (25), 465 (16), 439 (99), 407 (24), 301 (23); $MS^3 \rightarrow$ 465 (100), 573 (33), 555 (33), 453 (52), 447 (48), 327 (26), 301 (27)

Table 2. *(Continued)*

No.	Compound	Retention time (min)	Parent ion [M-H] *m/z*	Characteristic *m/z* of ions in negative ion mode
29	(Epi)gallocatechin-(4,8′/2,6′)-3′-*O*-galloyl(epi) gallocatechin	25.6	759	$MS^2 \rightarrow$ 407 (100), 591 (78), 573 (75), 455 (12), 423 (17) 289 (17); $MS^3 \rightarrow$ 285 (100), 389, 297, 283 (26), 267 (27), 256 (26), 243 (26); $MS^4 \rightarrow$ 257 (100), 213 (12)
30	3-*O*-Caffeoylquinic acid	13.2	353	$MS^2 \rightarrow$ 191 (100), 179 (45)
32	*Cis*-3-*O*-caffeoylquinic acid	14.4	353	$MS^2 \rightarrow$ 191 (100), 179 (50)
32	5-*O*-Caffeoylquinic acid	18.1	353	$MS^2 \rightarrow$ 191 (100)
33	*Cis*-5-*O*-caffeoylquinic acid	23.6	353	$MS^2 \rightarrow$ 191 (100)
34	3-*O*-*p*-Coumaroylquinic acid	18.9	337	$MS^2 \rightarrow$ 163 (100), 191 (10)
35	*Cis*-3-*O*-*p*-coumaroylquinic acid	20.1	337	$MS^2 \rightarrow$ 163 (100), 191 (10)
36	4-*O*-*p*-Coumaroylquinic acid	26.9	337	$MS^2 \rightarrow$ 173 (100)
37	*Cis*-4-*O*-*p*-coumaroylquinic acid	28.5	337	$MS^2 \rightarrow$ 173 (100)
38	5-*O*-*p*-Coumaroylquinic acid	24.8	337	$MS^2 \rightarrow$ 191 (100)
39	*Cis*-5-*O*-*p*-coumaroylquinic acid	30.4	337	$MS^2 \rightarrow$ 191 (100)
40	Catechin	16.6	289	$MS^2 \rightarrow$ 245 (100), 205 (45), 179 (13); $MS^3 \rightarrow$ 203 (100), 227 (27), 187 (22), 161 (13)
41	Epicatechin	23.7	289	$MS^2 \rightarrow$ 245 (100), 205 (38), 179 (10); $MS^3 \rightarrow$ 203 (100), 227 (25), 187 (25), 161 (16)
42	Gallocatechin	9.5	305	$MS^2 \rightarrow$ 179 (100), 261 (19), 221 (76), 219 (79), 165 (41), 125 (32); $MS^3 \rightarrow$ 164 (100), 151 (22), 135 (64), 120 (20)
43	Epigallocatechin	16.3	305	$MS^2 \rightarrow$ 179 (100), 261 (32), 221 (72), 219 (87), 165 (28), 125 (30); 164 (100), 151 (34), 135 (34)
44	Catechin gallate	33.5	441	$MS^2 \rightarrow$ 289 (100), 331 (10), 169 (10); 245 (100), 205 (58), 179 (20)
45	Epicatechin gallate	31.2	441	$MS^2 \rightarrow$ 289 (100), 331 (10), 169 (17); 245 (100), 205 (45), 179 (19)
46	Gallocatechin gallate	24.0	457	$MS^2 \rightarrow$ 169 (100), 331 (43), 305 (26), 193 (15)
47	Epigallocatechin gallate	23.0	457	$MS^2 \rightarrow$ 305 (100); $MS^2 \rightarrow$ 219 (100), 261, 221 (69), 204, 179, 165, 125
48	Quercetin-*O*-hexoside	36.9	463	$MS^2 \rightarrow$ 301 (100), 300 (30); $MS^3 \rightarrow$ 179 (100), 271 (52), 255 (25), 151 (90); $MS^4 \rightarrow$ 151 (100)
49	Quercetin-*O*-hexoside	35.8	463	$MS^2 \rightarrow$ 301 (100), 300 (50); $MS^3 \rightarrow$ 179 (100), 271 (62), 255 (36), 151 (90); $MS^4 \rightarrow$ 151 (100)
50	Quercetin-*O*-galloyl-hexoside	37.4	615	$MS^2 \rightarrow$ 463 (100), 301 (50); $MS^3 \rightarrow$ 301 (100), 300 (50); $MS^3 \rightarrow$ 179 (100), 271 (68), 255 (20), 151 (90)
51	Quercetin-*O*-pentoside	38.8	433	$MS^2 \rightarrow$ 301 (100); $MS^3 \rightarrow$ 179 (100), 151 (80); $MS^4 \rightarrow$ 151 (100)
52	Quercetin-*O*-rhamnoside	40.2	447	$MS^2 \rightarrow$ 301 (100), 300 (36); $MS^3 \rightarrow$ 179 (100), 271 (47), 255 (31), 151 (87); $MS^4 \rightarrow$ 151 (100)
53	Quercetin-*O*-pentoside-*O*-hexoside	43.7	595	$MS^2 \rightarrow$ 301 (100), 517 (32); $MS^3 \rightarrow$ 151 (100), 271 (15), 179 (80)
54	Quercetin-*O*-rhamnoside-*O*-hexoside	49.3	609	$MS^2 \rightarrow$ 301 (100), 541 (22), 463 (40); $MS^3 \rightarrow$ 179 (100), 273 (30), 151 (65)
55	Quercetin-*O*-rhamnoside-*O*-hexoside	51.0	609	$MS^2 \rightarrow$ 463 (100), 301 (32); $MS^3 \rightarrow$ 301 (100); $MS^3 \rightarrow$ 151 (100), 271 (95), 179 (98)
56	Quercetin-*O*-feruloyl-hexoside	52.4	639	$MS^2 \rightarrow$ 463 (100), 301 (35); $MS^3 \rightarrow$ 301 (100), 300 (50); $MS^3 \rightarrow$ 179 (100), 271 (40), 255 (50), 151 (38)
57	Quercetin-*O*-(*p*-hydroxy)benzoyl-hexoside	45.5	583	$MS^2 \rightarrow$ 463 (100), 301 (54); $MS^3 \rightarrow$ 301 (100), 300 (52); 151 (100), 271 (90), 255 (71), 179 (95)
58	Taxifolin-*O*-pentoside	35.3	435	$MS^2 \rightarrow$ 285 (100), 399 (78), 303 (50); $MS^3 \rightarrow$ 241 (100), 217 (35), 175 (60)
59	Myricetin-*O*-rhamnoside	30.9	463	$MS^2 \rightarrow$ 317 (100); $MS^3 \rightarrow$ 299 (100), 271 (95), 195 (30)
60	Myricetin-*O*-pentoside	34.5	—	$MS^2 \rightarrow$ 317 (100); $MS^3 \rightarrow$ 242 (100); 214 (60)
61	Myricetin-*O*-pentoside	35.0	—	$MS^2 \rightarrow$ 317 (100), 316 (50); $MS^3 \rightarrow$ 271 (100), 179 (30); $MS^3 \rightarrow$ 242 (100), 214 (22)

(Continues)

Table 2. *(Continued)*

No.	Compound	Retention time (min)	Parent ion [M-H] *m/z*	Characteristic *m/z* of ions in negative ion mode
62	Myricetin-*O*-hexoside	31.8	479	$MS^2 \rightarrow$ 317 (100), 316 (50); $MS^3 \rightarrow$ 271 (100), 179 (30)
63	Myricetin-*O*-hexoside	32.6	479	$MS^2 \rightarrow$ 331 (100), 316 (30); $MS^3 \rightarrow$ 271 (100), 270 (40), 287 (27), 270 (50), 179 (42); $MS^4 \rightarrow$ 243 (100), 242 (96), 214 (90), 158 (30)
64	Myricetin-*O*-hexoside	46.0	479	$MS^2 \rightarrow$ 331 (100), 316 (40); $MS^3 \rightarrow$ 271 (100), 270 (50), 287 (27), 270 (50), 179 (42); $MS^4 \rightarrow$ 243 (100), 242 (96), 214 (90), 158 (30)
65	Myricetin-*O*-galloyl-hexoside	30.9	631	$MS^2 \rightarrow$ 479 (100), 317 (30); 317 (100), 316 (60), 271 (10); $MS^3 \rightarrow$ 271 (100), 299 (91), 287 (43)
66	Myricetin-*O*-galloyl-hexoside	33.8	631	$MS^2 \rightarrow$ 479 (100), 317 (20); 316 (100); $MS^3 \rightarrow$ 271 (100), 287 (20), 179 (20)

Characterization of (epi)gallocatechin-(4,8′)-(epi)gallocatechin (M_r 610)

Three peaks were detected at *m/z* 609 in the EIC and the total ion chromatogram and were tentatively assigned as dimeric B-type PAs (**14–16**) with (epi)gallocatechin monomeric units (Fig. 6). For dimeric gallocatechin derivatives, alternative bisflavanol structures termed theasinensins need to be considered as well, which have been reported in black tea.[56,57] A comparison of MS^2 spectra of authentic theasinensin structures, however, shows that this class of compounds typically shows a base peak corresponding to a monomeric catechin unit and RDA fragment ions of low intensity, allowing unambiguous distinction between bisflavanols and PAs. They produced similar MS^n fragmentation patterns with similar intensities of ions. They produced the MS^2 base peak at *m/z* 423 ($[M\text{-}H^+\text{-}186\ Da]^-$) by the loss of an RDA fragment (168 Da) followed by the loss of a water molecule (18 Da); secondary peaks at *m/z* 305 ($[(epi)gallocatechin\text{-}H^+]^-$) originate from a QM fragment and at 441 ($[M\text{-}H^+\text{-}168\ Da]^-$) from an RDA fragment (Fig. 2). The presence of a QM fragment at *m/z* 305 showed that the top and base units are (epi)gallocatechin. From the preceding arguments, these PAs must have two (epi) gallocatechin units (Fig. 6).

Characterization of 3-*O*-galloyl-(epi)catechin-(4,8′)-(epi) catechin and (epi)catechin-(4,8′)-3′-*O*-galloyl-(epi)catechin (M_r 730)

Four peaks were detected at *m/z* 729 in the EIC and were tentatively assigned as gallates of the dimeric PAs with (epi)catechin monomeric units. Isomers **17** and **19** produced the MS^2 base peak at *m/z* 577 ($[M\text{-}H^+\text{-}152\ Da]^-$) by the loss of a galloyl residue; the secondary peaks were as follows: the peak at *m/z* 559 ($[M\text{-}H^+\text{-}170]^-$) resulted from the loss of a gallic acid; peaks at 451 ($[M\text{-}H^+\text{-}152\ Da\text{-}126\ Da]^-$) originated from an HRF fragment, at 425 ($[M\text{-}H^+\text{-}152\ Da\text{-}152]^-$) and 407 ($[M\text{-}H^+\text{-}152\ Da\text{-}170\ Da]^-$) from an RDA fragment, and at 289 ($[(epi)catechin\text{-}H^+]^-$) from a QM fragment (Figs 2, 3, and 7). They produced the MS^3 base peak at *m/z* 407 and secondary peaks at *m/z* 425 (RDA), 451 (HRF), and 289 (QM) (Figs 2, 3, and 7). Isomers **18** and **20** produced the MS^2 base peak at *m/z* 407 by the loss of a gallic acid (170 Da) and an RDA fragment (152 Da); secondary peaks at *m/z* 577 ($[M\text{-}H^+\text{-}152\ Da]^-$) resulted from the loss of a galloyl residue and at 559 ($[M\text{-}H^+\text{-}170]^-$) from the loss of a gallic acid; secondary peaks at 451 ($[M\text{-}H^+\text{-}152\ Da\text{-}126\ Da]^-$) originated from an HRF fragment, at 441 from an RDA fragment, and at 289 ($[(epi)catechin\text{-}H^+]^-$) from a QM fragment (Figs 2, 3, and 7).

There are two possibilities for the galloyl residue: either it is attached to the C3 of the top unit or to the C3′ of the base unit. If the galloyl residue is attached to the C3′ of the base unit, then it will favor the loss of gallic acid over the RDA fragment of the top unit, that is, formation of *m/z* 425 (Figs 2 and 3).[58] Hence, we observed an MS^2 base peak at *m/z* 407 and no secondary peak at *m/z* 425 (Figs 2, 3, and 7). In the second case, if the galloyl residue is attached to the C3 of the top unit, then it loses the galloyl residue and gallic acid and produces the MS^2 base peak at *m/z* 577 and a secondary peak at *m/z* 559, respectively. From the preceding arguments, isomers **17** and **19** were assigned as 3-*O*-galloyl-(epi)catechin-(4,8′)-(epi)catechin and **18** and **20** as (epi)catechin-(4,8′)-3′-*O*-galloyl-(epi)catechin.

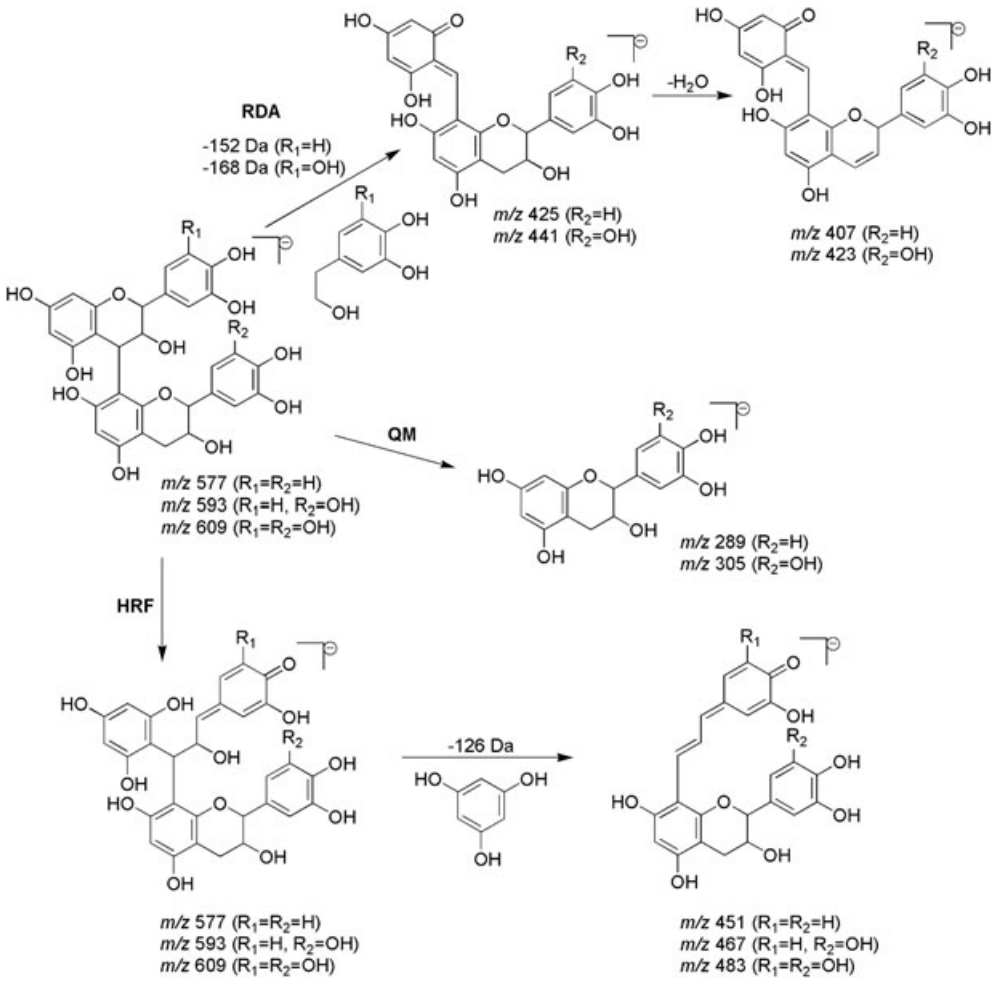

Figure 2. Fragmentation pathways of dimeric B-type PAs.

Characterization of (epi)gallocatechin-(4,8′)-3′-*O*-galloyl-(epi) catechin and 3-*O*-galloyl-(epi)catechin-(4,8′)-(epi)gallocatechin (M_r 746)

Three isomers were detected at *m/z* 745 and were tentatively assigned as gallates of (epi)gallocatechin-(epi)catechin. The first and third eluting isomers (**21** and **23**) produced the MS^2 base peak at *m/z* 407 ($[M\text{-}H^+\text{-gallic acid-168 Da}]^-$) (RDA) and secondary peaks at *m/z* 593 ($[M\text{-}H^+\text{-152 Da}]^-$) by the loss of a galloyl residue, at 575 ($[M\text{-}H^+\text{-170 Da}]^-$) by the loss of a gallic acid, at 559 and 467 from an HRF fragment, at 441 from an RDA fragment, at 423 from a dehydrated RDA, and at 289 ($[(epi)catechin\text{-}H^+]^-$) from a QM, which confirmed that the top unit is (epi)gallocatechin and the base unit is (epi)catechin (Figs 3 and 8). The presence of the MS^2 base peak at *m/z* 407 confirmed that the galloyl residue is attached to the C3′ of the base ring. Hence, isomers **21** and **23** were assigned as (epi)gallocatechin-(4,8′)-3′-*O*-galloyl-(epi)catechin.

The second eluting isomer **22** produced the MS^2 base peak at *m/z* 593 ($[M\text{-}H^+\text{-152 Da}]^-$) by the loss of a galloyl residue and secondary peaks at *m/z* 575 ($[M\text{-}H^+\text{-170 Da}]^-$) by the loss of a gallic acid, at 425 and 407 from an RDA fragment, and at 305 ($[(epi)gallocatechin\text{-}H^+]^-$) from a QM fragment, which confirmed that the top unit is (epi)catechin and the base unit is (epi)gallocatechin (Figs 3 and 8). The presence of the MS^2 base peak at *m/z* 593 confirmed that the galloyl residue is attached to C3 of the top unit (Fig. 3). From the preceding arguments, isomer **22** was assigned as 3-*O*-galloyl-(epi)catechin-(4,8′)-(epi)gallocatechin.

Characterization of (epi)gallocatechin-(4,8′)-3′-*O*-galloyl-(epi) gallocatechin (M_r 762)

Two isomers, **24** and **25**, were detected at *m/z* 761 and assigned as gallates of (epi)gallocatechin-(4,8′)-(epi)gallocatechin. They produced the MS^2 base peak at *m/z* 423 (RDA) and secondary peaks at *m/z* 609 by the loss of a galloyl residue, at 591 by the loss of a gallic acid, at 405 from an RDA fragment, and at 305 ($[(epi)gallocatechin\text{-}H^+]^-$) from a QM fragment, which confirmed the presence of (epi)gallocatechin-(4,8)-(epi)gallocatechin (Figs 2, , 3, and 9). The MS^2 base peak at *m/z* 423 also confirmed the presence of galloyl residue at the C3′ of the base unit. From the preceding points, isomers **24** and **25** were assigned as (epi) gallocatechin-(4,8′)-3′-*O*-galloyl-(epi)gallocatechin. It is worth mentioning that in black tea chemistry two epigallocatechins dimerize to furnish bis-flavans with a B-B-ring linkage also termed theasinensins.[59,60,56] The same linkage has also been observed in model oxidations with no PA-type structures reported.[56] Taking into account that this linkage has only been observed for the epigallocatechin stereochemistry, we can tentatively

Journal of MASS SPECTROMETRY

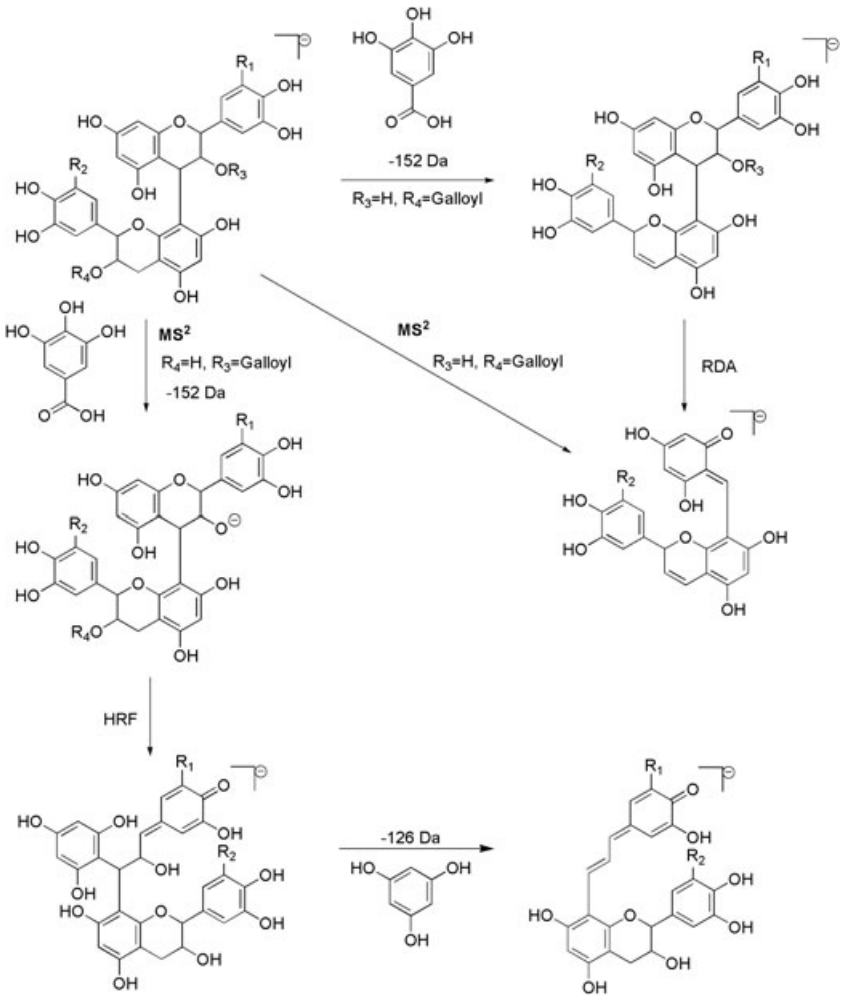

Figure 3. Fragmentation pathways of the gallates of dimeric B-type PAs.

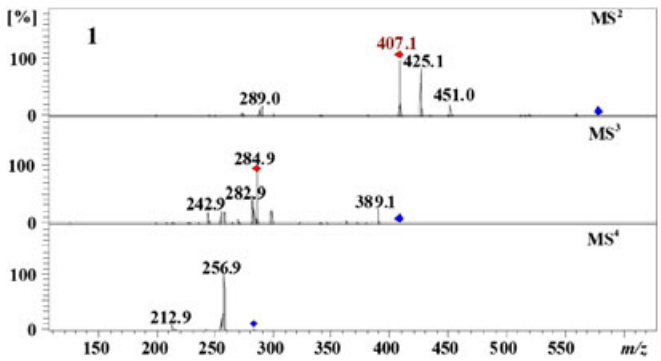

Figure 4. MS^4 spectra of compound **1** (**1–7** are identical) at *m/z* 577 in negative ion mode.

assign the compounds here with derivatives with at least one catechin moiety.

Characterization of (epi)catechin-(4,8′/2,6′)-(epi)catechin (M_r 576)

One peak was detected at *m/z* 575 and assigned as an A-type dimer of (epi)catechin unit. This compound **26** produced the MS^2 base peak at *m/z* 449 (HRF) and secondary peaks at *m/z* 539 ($[M\text{-}H^+\text{-}2H_2O]^-$), 423 (RDA), 407 (RDA), 327 (a benzofuran formation), and 289 and 285 (QMs) (Figs 10 and 11).[28]

Characterization of 3-*O*-galloyl-(epi)catechin-(4,8′/2,6′)-(epi) catechin (M_r 728)

One peak was detected at *m/z* 727 and was tentatively assigned as a gallate of an A-type dimeric (epi)catechin **27**. This compound produced the MS^2 base peak similar to isomers **17**, **19**, and **22** (Figs 7, 8, and 12) and could be easily assigned as 3-*O*-galloyl-(epi)catechin-(4,8′/2,6′)-(epi)catechin.

Characterization of 3-*O*-galloyl(epi)catechin-(4,8′/2,6′)-(epi) gallocatechin (M_r 744)

One peak was detected at *m/z* 743 and was tentatively assigned as a gallate of an A-type dimeric PA with (epi)catechin and (epi) gallocatechin **28**. This compound also produced the MS^2 base peak analogously to isomers **17**, **19**, and **22** (Figs 7 and 13) and could be easily assigned as 3-O-galloyl-(epi)catechin-(4,8′/2,6′)-(epi)gallocatechin.

Characterization of (epi)gallocatechin-(4,8′/2,6′)-3′-*O*-galloyl-(epi)gallocatechin (M_r 760)

One peak was detected at *m/z* 759 and was tentatively assigned as a gallate of an A-type dimeric (epi)gallocatechin **29**. This

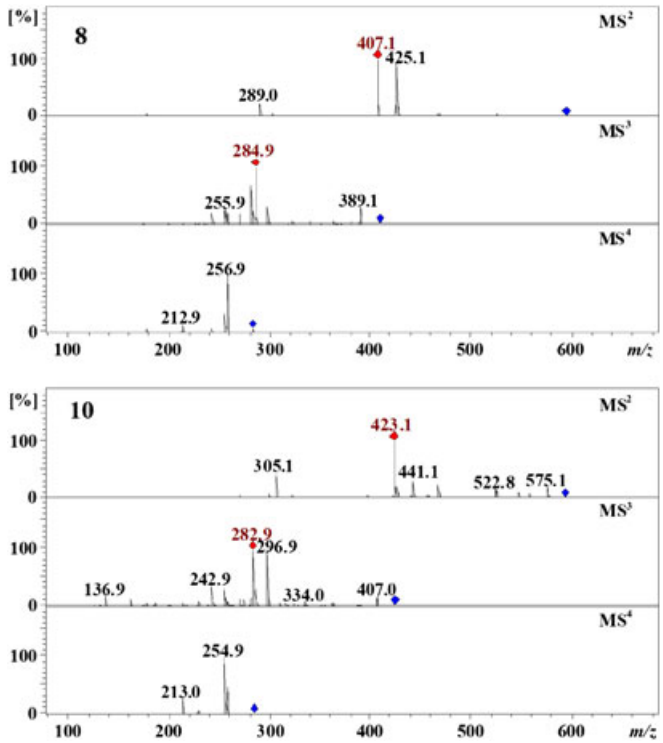

Figure 5. MS^4 spectra of compounds **8** (**8, 9, 11**, and **13** are identical) and **10** (**10** and **12** are identical) at *m/z* 593 in negative ion mode.

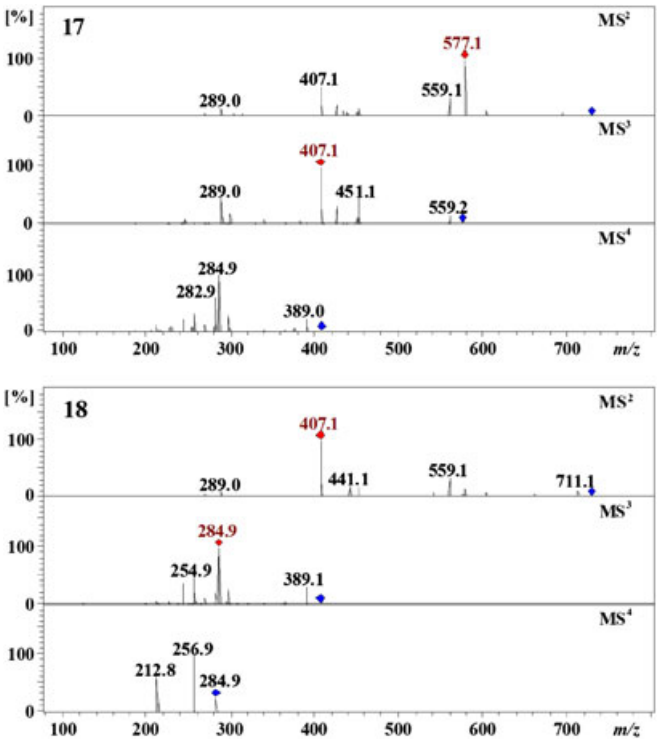

Figure 7. MS^4 spectra of compounds **17** (**17** and **19** are identical) and **18** (**18** and **20** are identical) at *m/z* 729 in negative ion mode.

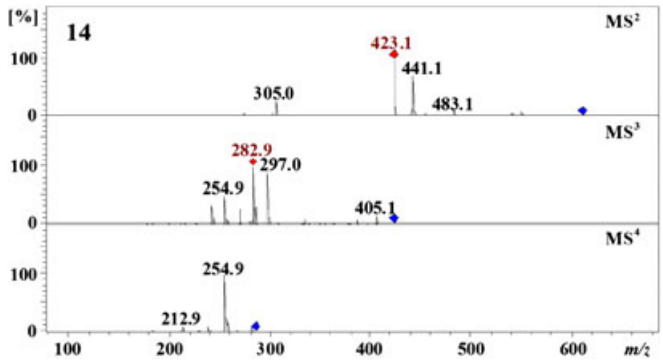

Figure 6. MS^4 spectra of compound **14** (**14–16** are identical) at *m/z* 609 in negative ion mode.

compound produced the MS^2 base peak analogous to isomers **18**, **20**, **21**, and **23–25** (Figs 7, 8, and 14) and could be easily assigned as (epi)gallocatechin-(4,8′/2,6′)-3′-*O*-galloyl-(epi)gallocatechin.

Identification of additional polyphenolic compounds

In addition to the PAs discussed in the preceding text, the chromatograms of the leaf samples revealed the presence of a series of further phenolic compounds, which were identified according to their high-resolution mass values, fragmentation patterns, UV–visible data, and retention times by comparison to literature data, mainly published previously by our group. Furthermore, four caffeoylquinic acids (**30–33**), six *p*-coumaroylquinic acids (**34–39**), epigallocatechin (**43**), gallocatechin (**42**), catechin (**40**), epicatechin (**41**), epigallocatechin gallate (**47**), catechin gallate (**44**), epicatechin gallate (**45**), gallocatechin

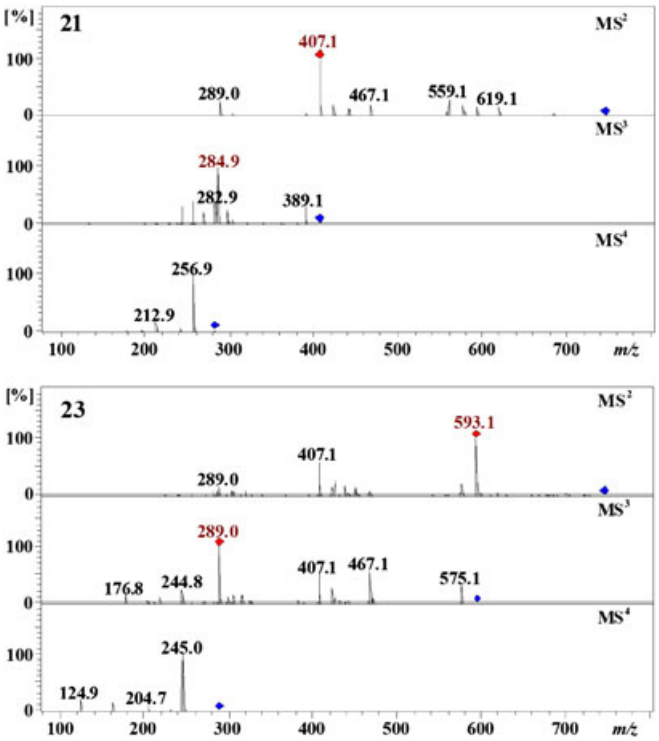

Figure 8. MS^4 spectra of compounds **21** (**21** and **22** are identical) and **23** at *m/z* 745 in negative ion mode.

gallate (**46**), two quercetin-*O*-hexosides (**48** and **49**), quercetin-*O*-galloyl-hexoside (**50**), quercetin-*O*-pentoside (**51**), quercetin-*O*-rhamnoside (**52**), quercetin-*O*-pentoside-*O*-hexoside (**53**), two

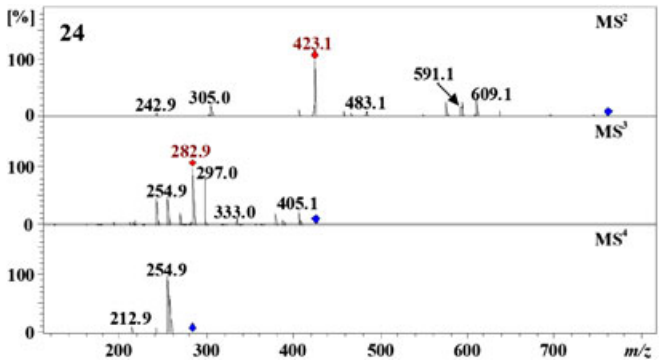

Figure 9. MS^4 spectra of compound **24** (**24** and **25** are identical) at *m/z* 761 in negative ion mode.

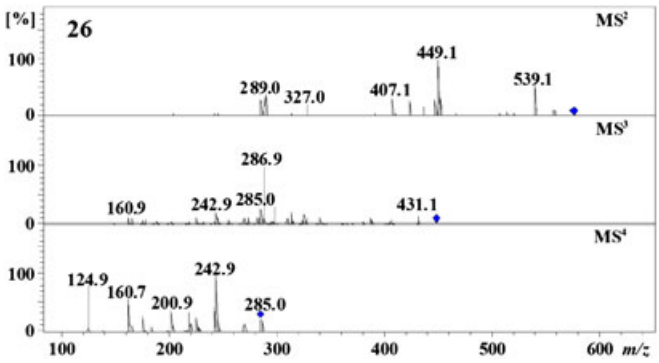

Figure 11. MS^4 spectra of compound **26** at *m/z* 575 in negative ion mode.

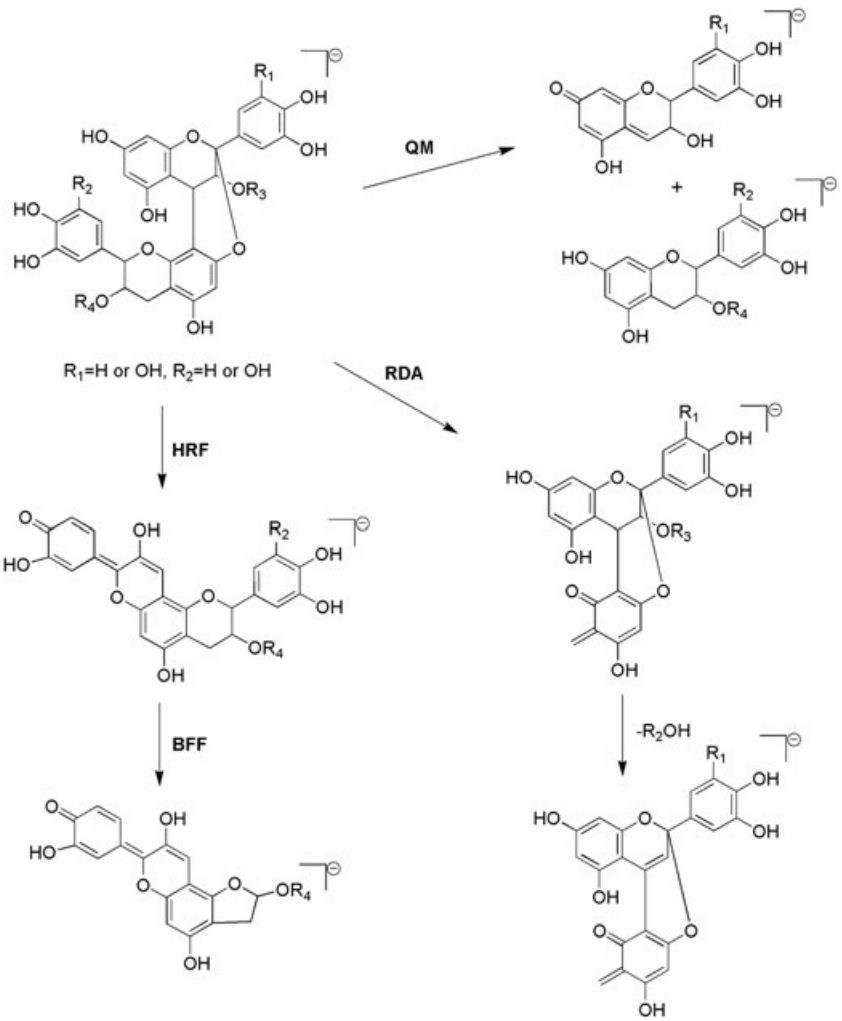

Figure 10. Fragmentation pathways of dimeric A-type PAs.

quercetin-*O*-rhamnoside-*O*-hexosides (**54** and **55**), quercetin-*O*-feruloyl-hexoside (**56**), quercetin-*O*-(*p*-hydroxy)benzoyl-hexoside (**57**), taxifolin-*O*-pentoside (**58**), myricetin-*O*-rhamnoside (**59**) two myricetin-*O*-pentosides (**60** and **61**), three myricetin-*O*-hexosides (**62–64**), and two myricetin-*O*-galloyl-hexosides (**65** and **66**) were detected, and they possess characteristic tandem MS spectra (Tables 1 and 2).[53,54,61–64]

CONCLUSIONS

We have shown that *Rhododendron* leaves are one of the richest sources of PAs reported in nature considering the number of individual derivatives present. We have for the first time compared a large number of different *Rhododendron* taxa, showing that the polyphenol profile of the 14 species and two cultivars investigated is remarkably similar.

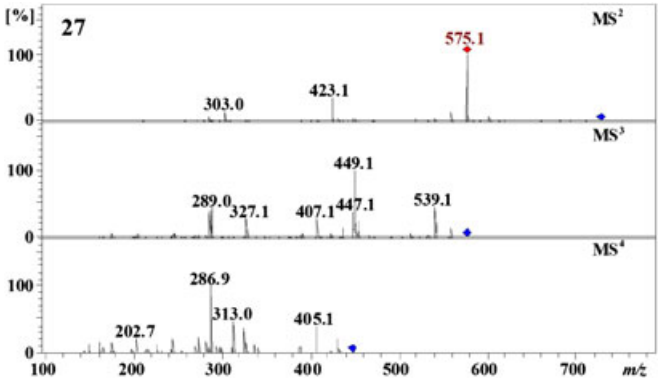

Figure 12. MS^4 spectra of compound **27** at *m/z* 727 in negative ion mode.

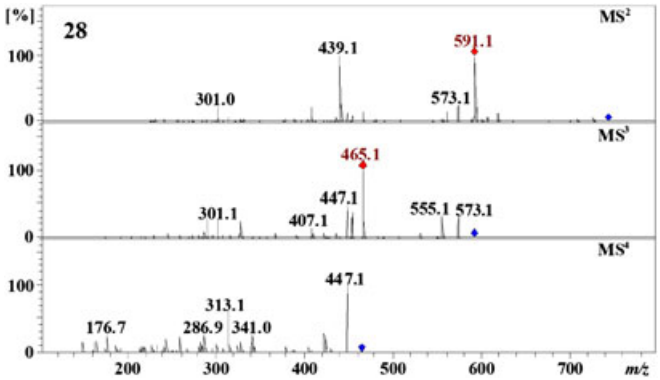

Figure 13. MS^4 spectra of compound **28** at *m/z* 743 in negative ion mode.

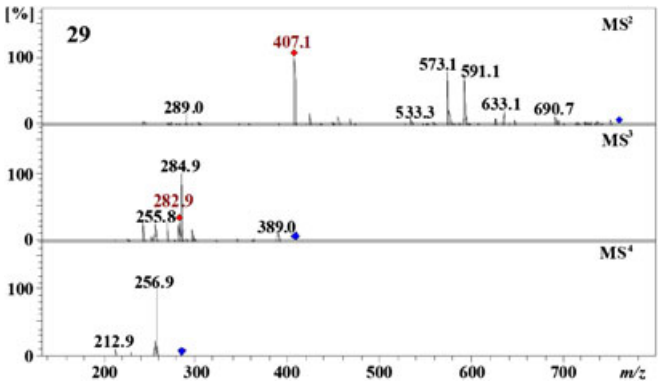

Figure 14. MS^4 spectra of compound **29** at *m/z* 759 in negative ion mode.

Twenty-nine dimeric PAs based on (epi)catechin and (epi) gallocatechin were detected and characterized on the basis of their unique fragmentation pattern in the negative ion mode tandem MS spectra, all of them for the first time from these sources, with ten of them previously not reported in nature. The position of the galloyl residue was assigned on the basis of the RDA fragmentation and the dehydrated RDA fragmentation; it resulted from the loss of gallic acid as a neutral loss in the negative ion mode. For the assignment of PA regiochemistry, we have proposed here for the first time a hierarchical key of negative ion mode data.

Acknowledgements

Financial support from Jacobs University Bremen and Alexander von Humboldt-Foundation is gratefully acknowledged. Furthermore, excellent technical support by Ms. Anja Müller is acknowledged. Provisions of *Rhododendron* samples from the Botanic Garden and Rhododendron-Park Bremen and botanical consultancy from Dr Hartwig Schepker are gratefully acknowledged.

REFERENCES

[1] R. W. Hemingway, J. J. Karchesy. Chemistry and Significance of Condensed Tannins. In Proceedings of the First North American Tannin Conference. Plenum Press: New York, **1989**, 553.
[2] Y. J. Hong, D. M. Barrett, A. E. Mitchell. Liquid chromatography/mass spectrometry investigation of the impact of thermal processing and storage on peach procyanidins. *J. Agric. Food Chem.* **2004**, *52*, 2366.
[3] W. G. Li, X. Y. Zhang, Y. J. Wu, X. Tian. Anti-inflammatory effect and mechanism of proanthocyanidins from grape seeds. *Acta Pharm. Sinic.* **2001**, *22*, 1117.
[4] H. G. Preuss, D. Bagchi, M. Bagchi. Protective effects of a novel niacin-bound chromium complex and a grape seed proanthocyanidin extract on advancing age and various aspects of syndrome X. *Ann. N. Y. Acad. Sci.* **2002**, *957*, 250.
[5] K. M. Kalili, A. de Villiers. Off-line comprehensive two-dimensional hydrophilic interaction × reversed phase liquid chromatographic analysis of green tea phenolics. *J. Sep. Sci.* **2010**, *33*, 853.
[6] M. H. Omar, W. Mullen, A. Crozier. Identification of proanthocyanidin dimers and trimers, flavone c-glycosides, and antioxidants in *Ficus deltoidea*, a Malaysian herbal tea. *J. Agric. Food Chem.* **2011**, *59*, 1363.
[7] J. M. Awika, L. Dykes, L. W. Gu, L. W. Rooney, R. Prior. Effect of processing on molecular weight distribution and antioxidant properties of sorghum proanthocyanidins. *Abstr. Papers Am. Chem. Soc.* **2004**, *228*, 084.
[8] D. Bagchi, A. Garg, R. L. Krohn, M. Bagchi, M. X. Tran, S. J. Stohs. Oxygen free radical scavenging abilities of vitamins C and E, and a grape seed proanthocyanidin extract *in vitro*. *Res. Commun. Mol. Path.* **1997**, *95*, 179.
[9] M. Serafini, G. Maiani, A. Ferro-Luzzi. Alcohol-free red wine enhances plasma antioxidant capacity in humans. *J. Nutr.* **1998**, *128*, 1003.
[10] S. S. Joshi, C. A. Kuszynski, M. Bagchi, D. Bagchi. Chemopreventive effects of grape seed proanthocyanidin extract on Chang liver cells. *Toxicology* **2000**, *155*, 83.
[11] J. A. Bomser, K. W. Singletary, M. A. Wallig, M. A. L. Smith. Inhibition of TPA-induced tumor promotion in CD-1 mouse epidermis by a polyphenolic fraction from grape seeds. *Cancer Lett.* **1999**, *135*, 151.
[12] X. Ye, R. L. Krohn, W. Liu, S. S. Joshi, C. A. Kuszynski, T. R. McGinn, M. Bagchi, H. G. Preuss, S. J. Stohs, D. Bagchi. The cytotoxic effects of a novel IH636 grape seed proanthocyanidin extract on cultured human cancer cells. *Mol. Cell. Biochem.* **1999**, *196*, 99.
[13] H. G. Preuss, S. Montamarry, B. Echard, R. Scheckenbach, D. Bagchi. Long-term effects of chromium, grape seed extract, and zinc on various metabolic parameters of rats. *Mol. Cell. Biochem.* **2001**, *223*, 95.
[14] E. Bayeta, B. H. S. Lau. Pycnogenol inhibits generation of inflammatory mediators in macrophages. *Nutr. Res.* **2000**, *20*, 249.
[15] N. Erdemoglu, E. K. Akkol, E. Yesilada, I. Calis. Bioassay-guided isolation of anti-inflammatory and antinociceptive principles from a folk remedy, *Rhododendron ponticum* L. leaves. *J. Ethnopharmacol.* **2008**, *119*, 172.
[16] J. L. He, Y. Z. Chen, M. Farzan, H. Y. Choe, A. Ohagen, S. Gartner, J. Busciglio, X. Y. Yang, W. Hofmann, W. Newman, C. R. Mackay, J. Sodroski, D. Gabuzda. CCR3 and CCR5 are co-receptors for HIV-1 infection of microglia. *Nature* **1997**, *385*, 645.
[17] M. B. Witte, F. J. Thornton, D. T. Efron, A. Barbul. Enhancement of fibroblast collagen synthesis by nitric oxide. *Nitric Oxide-Biol. Chem.* **2000**, *4*, 572.
[18] D. K. Das, M. Sato, P. S. Ray, G. Maulik, R. M. Engelman, A. A. E. Bertelli, A. Bertelli. Cardioprotection of red wine: role of polyphenolic antioxidants. *Drug. Exp. Clin. Res.* **1999**, *25*, 115.
[19] P. Delacroix. Double-blind trial of endotelon in chronic venous insufficiency. *Rev. Med. Paris* **1981**, *22*, 1793.
[20] E. N. Frankel, J. Kanner, J. B. German, E. Parks, J. E. Kinsella. Inhibition of oxidation of human low-density-lipoprotein by phenolic substances in red wine. *Lancet* **1993**, *341*, 454.

[21] Z. Ni, Y. Mu, O. Gulati. Treatment of melasma with Pycnogenol®. *Phytother. Res.* **2002**, *16*, 567–571.
[22] D. Bagchi, S. D. Ray, D. Patel, M. Bagchi. Protection against drug- and chemical-induced multiorgan toxicity by a novel IH636 grape seed proanthocyanidin extract. *Drug. Exp. Clin. Res.* **2001**, *27*, 3.
[23] G. J. Fisher, S. C. Datta, H. S. Talwar, Z. Q. Wang, J. Varani, S. Kang, J. J. Voorhees. Molecular basis of sun-induced premature skin ageing and retinoid antagonism. *Nature* **1996**, *379*, 335.
[24] C. Saliou, G. Rimbach, H. Moini, L. McLaughlin, S. Hosseini, J. Lee, R. R. Watson, L. Packer. Solar ultraviolet-induced erythema in human skin and nuclear factor-kappa-B-dependent gene expression in keratinocytes are modulated by a French maritime pine bark extract. *Free Radical Bio. Med.* **2001**, *30*, 154.
[25] B. H. S. Lau, S. K. Riesen, K. P. Truong, E. W. Lau, P. Rohdewald, R. A. Barreta. Pycnogenol® as an adjunct in the management of childhood asthma. *J. Asthma* **2004**, *41*, 825.
[26] C. Santos-Buelga, A. Scalabert. Proanthocyanidins and tannin-like compounds—nature, occurrence, dietary intake and effects on nutrition and health. *J. Sci. Food Agr.* **2000**, *80*, 1094.
[27] F. Tayeau, J. Masquelier. Les pigments de la graine d'arachide- le chromogene constitution chimique et physiologique. *Bull. Soc. Chim. France* **1949**, *31*, 72–75
[28] L. W. Gu, M. A. Kelm, J. F. Hammerstone, Z. Zhang, G. Beecher, J. Holden, D. Haytowitz, R. L. Prior. Liquid chromatographic/electrospray ionization mass spectrometric studies of proanthocyanidins in foods. *J. Mass Spectrom.* **2003**, *38*, 1272.
[29] H.-J. Li, M. L. Deinzer. Tandem mass spectrometry for sequencing proanthocyanidins. *Anal. Chem.* **2007**, *79*, 1739.
[30] J. B. Harborne. Flavonoid patterns and phytogeography—the genus *Rhododendron* section *Vireya*. *Phytochemistry* **1986**, *25*, 1641.
[31] M. H. Yang, J. G. Luo, X. F. Huang, L. Y. Kong. Flavonol glycosides with –D-aldohexoses from *Rhododendron irroratum*. *Nat. Prod. Res.* **2010**, *24*, 920.
[32] J. B. Harborne, C. A. Williams. Leaf survey of flavonoids and simple phenols in the genus Rhododendron. *Phytochemistry* **1971**, *10*, 2727.
[33] N. Sharma, U. K. Sharma, A. P. Gupta, A. K. Sinha. Simultaneous determination of epicatechin, syringic acid, quercetin-3-O-galactoside and quercitrin in the leaves of Rhododendron species by using a validated HPTLC method. *J. Food Comp. Anal.* **2010**, *23*, 214.
[34] M. H. Yang, L. Y. Kong. Flavonols and flavonol glycosides from Rhododendron irroratum. *Chem. Nat. Comp.* **2008**, *44*, 98.
[35] R. P. Doss, W. H. Hatheway, B. F. Hrutfiord. Composition of essential oils of some lipidote Rhododendrons. *Phytochemistry* **1986**, *25*, 1637.
[36] C. X. Zhao, X. N. Li, Y. Z. Liang, H. Z. Fang, L. F. Huang, F. Q. Guo. Comparative analysis of chemical components of essential oils from different samples of Rhododendron with the help of chemometrics methods. *Chemometr Intell. Lab.* **2006**, *82*, 218.
[37] G. Chen, H. Z. Jin, X. F. Li, Q. Zhang, Y. H. Shen, S. K. Yan, W. D. Zhang. A new chromone glycoside from *Rhododendron spinuliferum*. *Arch. Pharm. Res.* **2008**, *31*, 970.
[38] Y. Kashiwada, K. Yamazaki, Y. Ikeshiro, T. Yamagishi, T. Fujioka, K. Mihashi, K. Mizuki, L. M. Cosentino, K. Fowke, S. L. Morris-Natschke, K.-H. Lee. Isolation of rhododaurichromanic acid B and the anti-HIV principles rhododaurichromanic acid A and rhododaurichromenic acid from *Rhododendron dauricum*. *Tetrahedron* **2001**, *57*, 1559.
[39] D. Evans, B. A. Knights, V. B. Math, A. L. Ritchie. β-Diketones in *Rhododendron* waxes. *Phytochemistry* **1975**, *14*, 2447–2451.
[40] C. Q. Fan, W. M. Zhao, B. Y. Ding, G. W. Qin. Constituents from the leaves of *Rhododendron latoucheae*. *Fitoterapia* **2001**, *72*, 449–452.
[41] M. A. Tantry, R. Khan, S. Akbar, A. R. Dar, A. S. Shawl, M. S. Alam. An unusual bioactive oleanane triterpenoid from *Rhododendron campanulatum* D. Don. *Chinese Chem. Lett.* **2011**, *22*, 575.
[42] S. J. Wang, S. Lin, C. G. Zhu, Y. C. Yang, S. A. Li, J. J. Zhang, X. G. Chen, J. G. Shi. Highly acylated diterpenoids with a new 3,4-secograyanane skeleton from the flower buds of *Rhododendron molle*. *Org. Lett.* **2010**, *12*, 1560.
[43] W. D. Zhang, H. Z. Jin, G. Chen, X. F. Li, S. K. Yan, L. Zhang, Y. H. Shen, M. Yang. A new grayanane diterpenoid from *Rhododendron decorum*. *Fitoterapia* **2008**, *79*, 602.
[44] J. Sakakibara, T. Kaiya. Terpenoids of *Rhododendron japonicum*. *Phytochemistry* **1983**, *22*, 2547.
[45] J. H. Block, G. H. Constant Jr. Revised structure of a steroid oxide from *Rhododendron macrophyllum*. *Phytochemistry* **1972**, *11*, 3279.
[46] S. N. Chen, H. P. Zhang, L. Q. Wang, G. H. Bao, G. W. Qin. Diterpenoids from the flowers of *Rhododendron molle*. *J. Nat. Prod.* **2004**, *67*, 1903.
[47] J. A. Klocke, M. Y. Hu, S. F. Chiu, I. Kubo. Grayanoid diterpene insect antifeedants and insecticides from *Rhododendron molle*. *Phytochemistry* **1991**, *30*, 1797.
[48] D. M. Gibson. Rhododendron, a study. *Br. Homoeopath. J.* **1971**, *60*, 294.
[49] T. Prakash, S. D. Fadadu, U. R. Sharma, V. Surendra, D. Goli, P. Stamina, D. Kotresha. Hepatoprotective activity of leaves of *Rhododendron arboreum* in CCl_4 induced hepatotoxicity in rats. *J. Med. Plants Res.* **2008**, *2*, 315.
[50] S. H. Lee, S. A. Sancheti, M. R. Bafna, S. S. Sancheti, S. Y. Seo. Acetylcholinesterase inhibitory and antioxidant properties of *Rhododendron yedoense* var. poukhanense bark. *J. Med. Plants Res.* **2011**, *5*, 248.
[51] S. Silici, O. Sagdic, L. Ekici. Total phenolic content, antiradical, antioxidant and antimicrobial activities of *Rhododendron* honeys. *Food Chem.* **2010**, *121*, 238.
[52] K. Gescher, W. Hafezi, A. Louis, J. Kuhn, A. Hensel. Anti-herpes simplex virus type 1 activity of *Rhododendron ferrugineum* L. extracts. *Planta Med.* **2009**, *75*, 989.
[53] R. Jaiswal, N. Kuhnert. Determination of the hydroxycinnamate profile of 12 members of the *Asteraceae* family. *Phytochemistry* **2011**, *72*, 781.
[54] R. Jaiswal, S. Deshpande, N. Kuhnert. Profiling the chlorogenic acids of *Rudbeckia hirta*, *Helianthus tuberosus*, *Carlina acaulis* and *Symphyotrichum novae-angliae* leaves by LC–MS^n. *Phytochem. Anal.* **2011**, *22*, doi: 10.1002/pca.1299.
[55] L. J. Porter. Flavans and proanthocyanidins. In The Flavonoids: Advances in Research Since 1980, J. B. Harborne (Ed.). Chapman & Hall: London, **1988**, 21–62.
[56] J. W. Drynan, M. N. Clifford, J. Obuchowicz, N. Kuhnert. The chemistry of low molecular weight black tea polyphenols. *Nat. Prod. Rep.* **2010**, *27*, 417.
[57] N. Kuhnert. Unraveling the structure of the black tea thearubigins. *Arch. Biochem. Biophys.* **2010**, *501*, 37.
[58] R.-J. Lee, V. S. Y. Lee, J. T. C. Tzen, M.-R. Lee. Study of the release of gallic acid from (−)-epigallocatechin gallate in old oolong tea by mass spectrometry. *Rapid Commun. Mass Spectrom.* **2010**, *24*, 851.
[59] R. Jaiswal, M. F. Matei, F. Ullrich, N. Kuhnert. How to distinguish between caffeoylshikimate esters and chlorogenic acid lactones by liquid chromatography–tandem mass spectrometry. *J. Mass Spectrom.***2011**, *46*, 933–942.
[60] N. Kuhnert, J. Obuchowicz, W. J. Drynan, M. N. Clifford. On the chemical characterization of black tea thearubigins using mass spectrometry. *Rapid Commun. Mass Spectrom.* **2010**, *24*, 3387–3404.
[61] M. J. Cho, L. R. Howard, R. L. Prior, J. R. Clark. Flavonol glycosides and antioxidant capacity of various blackberry and blueberry genotypes determined by high-performance liquid chromatography/mass spectrometry. *J. Sci. Food Agr.* **2005**, *85*, 2149.
[62] S. C. Gouveia, P. C. Castilho. Characterization of phenolic compounds in *Helichrysum melaleucum* by high-performance liquid chromatography with on-line ultraviolet and mass spectrometry detection. *Rapid Commun. Mass Spectrom.* **2010**, *24*, 1851.
[63] E. Hvattum. Determination of phenolic compounds in rose hip (*Rosa canina*) using liquid chromatography coupled to electrospray ionisation tandem mass spectrometry and diode-array detection. *Rapid Commun. Mass Spectrom.* **2002**, *16*, 655.
[64] I. O. Vvedenskaya, R. T. Rosen, J. E. Guido, D. J. Russell, K. A. Mills, N. Vorsa. Characterization of flavonols in cranberry (*Vaccinium macrocarpon*) powder. *J. Agr. Food Chem.* **2004**, *52*, 188.